International Journal of Environmental Science and Technology (2026) 23:611
https://doi.org/10.1007/s13762-026-07412-w

ORIGINAL PAPER

Nitrogen-to-phosphorus limitation shift in a polyhydroxyalkanoate-enriched mixed microbial community

S. Falcioni[1] · L. Di Gloria[2] · A. Manmeen[3] · E. Touloupakis[4] · M. Ramazzotti[2] · M. E. Suárez-Ojeda[5] · D. Gabriel[5] · G. Munz[1]

Received: 24 November 2025 / Revised: 8 June 2026 / Accepted: 9 August 2026 / Published online: 31 August 2026
© The Author(s) 2026

Abstract

Polyhydroxyalkanoates are biodegradable polyesters considered promising alternatives to conventional plastics. To reduce costs associated with pure cultures, increasing attention has been given to mixed microbial communities and low-cost substrates. Uncoupled feeding of carbon and nutrients enables the separation of growth and polyhydroxyalkanoates accumulation phase and has been reported as a strategy to enhance process performance. While nitrogen limitation is usually applied to restrict biomass growth, phosphorus limitation has been also proposed as a relevant alternative limiting condition. This study investigates the sequential transition from nitrogen- to phosphorus-limiting conditions in a single sequential batch reactor, with emphasis on temporal process evolution and microbial community dynamics. Nitrogen limitation was associated with higher polyhydroxybutyrate accumulation than phosphorus limitation conditions. Low phosphorus availability may have been associated with intracellular phosphorus storage or retention, potentially affecting the uncoupled feeding regime, or metabolic energy redirection mechanisms that may have reduced accumulation. Filamentous polyhydroxyalkanoates-accumulating bacteria (e.g., *Neomegalonema*) dominated under nitrogen limitation, whereas *Thauera* and *Paracoccus* increased under phosphorus-limiting conditions.

Editorial responsibility: Samareh Mirkia.

✉ D. Gabriel
David.Gabriel@uab.cat

[1] Department of Civil and Environmental Engineering, University of Florence, Florence, Italy

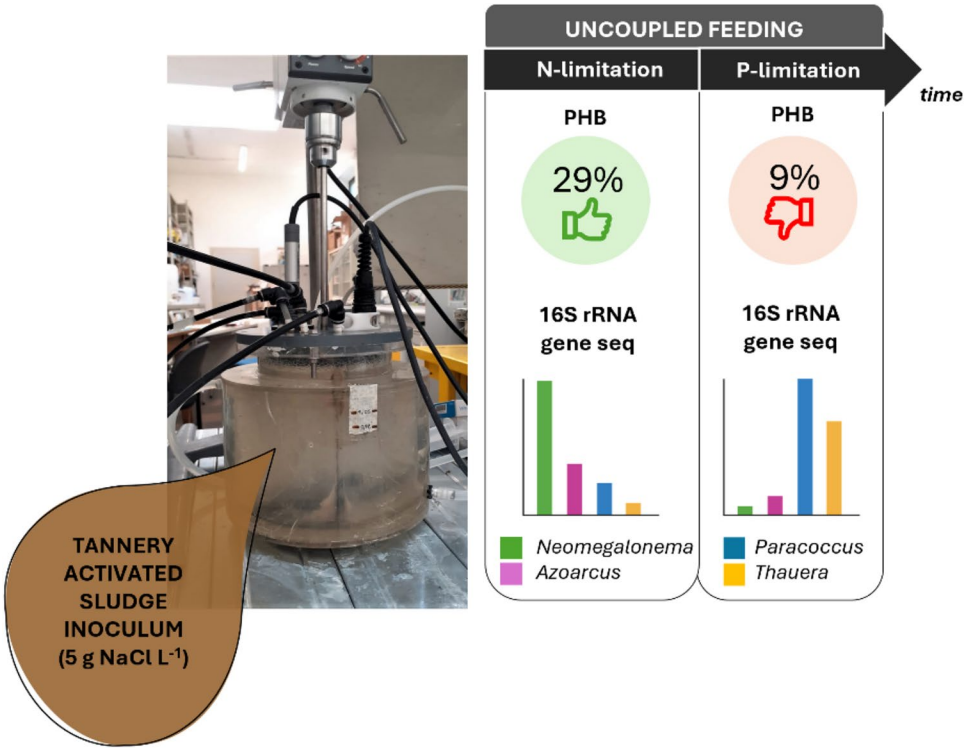
[2] Department of Clinical and Experimental Biomedical Sciences, University of Florence, Florence, Italy

[3] Energy Technology Program, Faculty of Engineering, Prince of Songkla University, Songkhla, Thailand

[4] Research Institute on Terrestrial Ecosystems, National Research Council, Sesto Fiorentino, Italy

[5] GENOCOV Research Group, Department of Chemical, Biological and Environmental Engineering, School of Engineering, Universitat Autònoma de Barcelona, Bellaterra, Spain

Graphical abstract



Keywords Polyhydroxyalkanoates · Mixed microbial communities · Uncoupled feeding strategy · Nutrient limitation · *Neomegalonema* · Microbiota

Introduction

Polyhydroxyalkanoates (PHA) are biodegradable polyesters considered promising alternatives to conventional plastics such as polypropylene and polyethylene (Rosenboom et al. 2022; Mai et al. 2024). Their increasing relevance is driven by their broad potential applications, particularly in medical and agricultural sectors, as well as their intrinsic biodegradability (Zhou et al. 2023; Jayalath and Alwis 2025). PHA are intracellular, water-insoluble carbon and energy storage granules accumulated by many bacteria as cytoplasmic inclusion bodies (Estévez-Alonso et al. 2021; Mai et al. 2024). To date, more than 150 PHAs have been identified, differing in monomer composition and chain length. Among them, poly(3-hydroxybutyrate) (PHB) is the most widespread homopolymer and the first industrially produced PHA (Zhou et al. 2023; Zhang et al. 2024).

Among selective strategies, Aerobic Dynamic Feeding (ADF), also know as feast-and-famine, is widely applied to enrich PHA-accumulating communities. In this system, alternating carbon excess and scarcity selects for microorganisms capable of storing carbon as PHA during feast and consume it during famine, leading to competitive enrichment of storage organisms. PHA content up to 91% of dry cell weight have been reported under optimized conditions (Coats et al. 2016). However, overall productivity in MMC-based systems, 1.2 g PHA L^{-1} h^{-1}, remains lower than in pure cultures, 3 g PHA L^{-1} h^{-1} (Mannina et al. 2020). To improve performance, uncoupled feeding strategy (UF) has been proposed, in which carbon and nutrients are supplied separately to decouple growth from storage. This typically involves: (1) a carbon (C)-rich, nutrient-poor source and (2) a C-poor, nutrient-rich source (Altun 2019).

Silva et al. (2017) first demonstrated that decoupling nitrogen and carbon supply in a PHA-accumulating culture fed with acetic and propionic acids could double the bioreactor productivity. Almost simultaneously, Oliveira et al. (2017) showed that the UF strategy also promoted the selection of a more efficient PHA-storing culture when using complex feedstocks containing readily biodegradable substrates. Subsequent studies have investigated the effects of organic loading rate (OLR), sludge retention time (SRT), pH control (Oliveira et al. 2017; Crognale et al. 2019; Lorini et al. 2020; Matos et al. 2021; Khor et al. 2023) and minor process adjustments to enhance performance (Chen et al. 2015; Argiz et al. 2020; Cruz et al. 2022).

In most PHA production systems, nitrogen (N) limitation is commonly applied to restrict biomass growth. However, in full-scale wastewater treatment contexts, phosphorus (P) limitation can also occur due to its chemical precipitation and crystallization (Korkakaki et al. 2017). Despite this relevance, relatively few studies have investigated P-limiting conditions (Cavaillé et al. 2016; Korkakaki et al. 2017; Brison et al. 2022; Di Caprio 2022) or comparison between N- and P-limiting conditions (Montiel-Jarillo et al. 2017; Stouten 2021).

In this study, a sequential experimental strategy was applied to investigate the transition from N- to P-limiting conditions in a single sequential batch reactor (SBR). This design allows the observation of temporal dynamics and microbial adaptation within the same enriched community under changing operational conditions, rather than a strict parallel comparison between independent systems. Besides, instead of focusing on single bacteria already well-known to be related to PHA production (e.g. *Thauera*, *Paracoccus* or *Azoarcus*) (Coats et al. 2016; Wang et al. 2017; Carvalho et al. 2022; Correa-Galeote et al. 2022), microbial community dynamics were assessed using 16S rRNA gene amplicon sequencing with universal primers, enabling a characterization of the overall microbial community.

A secondary aspect of this study explores the use of activated sludge from a tannery wastewater treatment plant cultivated under mild salinity conditions (5 g NaCl L^{-1}) as inoculum. While tannery effluents are characterized by the presence of complex and potentially inhibitory compounds such as sulphides and tannins (Munz et al. 2008), microbial communities adapted to such environments may exhibit increased profile stability or, at least, functional redundancy. Mild salinity may act as a selective pressure favouring halotolerant bacteria, potentially relevant for PHA-accumulating systems (Wen et al. 2024). However, the effects of salinity remain not directly quantified in this study. Rather, this study contributes to expanding the range of viable inocula and demonstrates the feasibility of leverage them in applied contexts.

Finally, the objective of this work was to evaluate PHB production and microbial community dynamics in a MMC enriched from tannery wastewater under UF conditions. Specifically, the study aimed to: (i) assess the temporal response to sequential N- and P-limiting conditions, (ii) characterize associated microbial community shifts using 16S rRNA gene amplicon sequencing, and (iii) explore the potential of saline-adapted inocula for PHA production in engineered systems.

The study was carried out at the University of Florence, Florence, Italy, from May 2022 to July 2023.

Materials and methods

SBR set up and operating conditions

The MMCs were enriched in PHA-accumulating microorganisms using a single plexiglass sequencing batch reactor (SBR) with an effective maximum working volume of 1.3 L. The SBR was inoculated with activated sludge collected from a municipal and tannery wastewater treatment plant (WWTP) operated by Consorzio Cuoiodepur S.p.A. (Tuscany, Italy). The reactor was operated sequentially under N-limiting conditions (period I, 0–314 days) followed by P-limiting conditions (period II, 315–409 days).

Given the single-reactor configuration, this sequential design inherently implies that nutrient effects are not independent of time and microbial adaptation; therefore, the observed responses should be interpreted as combined effects of changing selective pressures and system evolution over time rather than as strictly independent effects of N and P limitation.

An UF strategy was applied throughout SBR operation, consisting of alternating phases: (i) a PHA accumulation phase, during which carbon was supplied in the absence of external nutrients, and (ii) a growth phase, during which nutrients were supplied while previously accumulated PHA served as carbon source for biomass growth. To minimize overlap between phases, nutrient concentrations were designed to be limiting relative to the applied carbon load, based on theoretical calculations (see Supplementary Material). Proper selective conditions were operationally defined when residual N or P concentrations at the end of each cycle (last 0.5–1 h) remained below 0.5 mg L^{-1} and 0.05 mg L^{-1}, respectively. The N and P thresholds were set based on stoichiometric nutrient-to-C requirements, at less than 5% of the influent concentrations for both N and P.

A settling phase followed by supernatant discharge was implemented as a physical selection pressure to rapidly enrich PHA-accumulating microorganisms (Chen et al. 2015). Additionally, controlled sludge wasting was applied at the end of each cycle to keep constant the SRT and to reinforce the selection pressure towards PHA-accumulating bacteria (Cruz et al. 2022).

The reactor configuration and operational cycle are illustrated in Fig. 1A and Fig. 1B, respectively. Each 12-h cycle comprises the following phases: carbon feeding (0.4 L), accumulation phase, settling, supernatant discharge (0.4 L), nutrient feeding (0.1 L), growth phase, sludge purging (0.1 L). Additionally, an intermediate mixing and aeration phase was included between supernatant discharge and nutrient feeding to ensure fully aerobic conditions during the growth phase.

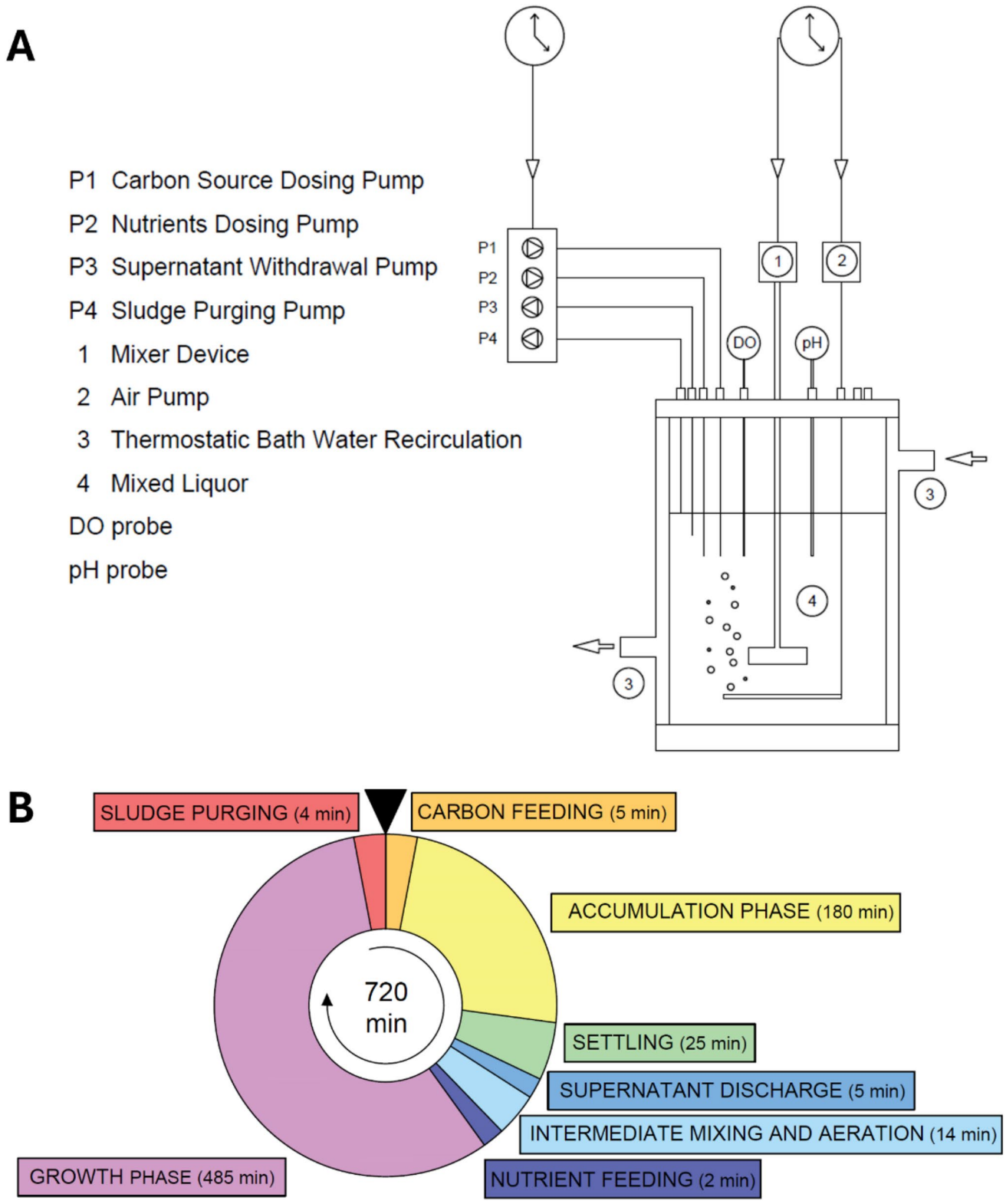


Fig. 1 Lab-scale SBR: schematic (**A**) and operating cycle (**B**)

The SBR was fed with two distinct synthetic solutions, one containing the carbon source, 80% acetate and 20% propionate (on chemical oxygen demand -COD- basis), and another one consisting of nutrients and micronutrients. The mineral medium solution was adapted from (Palmeiro-Sánchez et al. 2016a) and comprised the following constituents: NH_4Cl (1157.9 mg L^{-1}), KH_2PO_4 (204.0 mg L^{-1}), K_2HPO_4 (164.7 mg L^{-1}), $MgSO_4{\cdot}7H_2O$ (83.7 mg L^{-1}), KCl (32.7 mg L^{-1}), Allylthiourea (61.5 mg L^{-1}), EDTA Triplex III (117.7 mg L^{-1}), $ZnSO_4{\bullet}7H_2O$ (40.5 mg L^{-1}), $CaCl_2$ (15.2 mg L^{-1}), $MnCl_2{\cdot}4H_2O$ (9.2 mg L^{-1}), $FeCl_2{\cdot}4H_2O$ (6.4 mg L^{-1}), $CoCl_2{\cdot}6H_2O$ (2.6 mg L^{-1}), $CuSO_4{\cdot}5H_2O$ (2.6 mg L^{-1}), $(NH_4)6MO_7O_{24}{\cdot}4H_2O$ (2.6 mg L^{-1}). Allylthiourea (ATU) was added to avoid nitrification. The absence of nitrites and nitrates was periodically checked. The amount of each P sources (KH_2PO_4 and K_2HPO_4) was adjusted to maintain the solution pH to 7.

Under P-limiting conditions (Period II), the composition of the mineral medium was kept identical to that used under N-limiting conditions (Period I), as were the cycle structure and operational parameters, with the exception of N and P concentrations. To establish P instead of N limitation, the N concentration was increased (NH_4Cl = 1201.6 mg L^{-1}), while P concentration was reduced (KH_2PO_4 = 108.8 mg L^{-1}, K_2HPO_4 = 87.8 mg L^{-1}), in order to shift the limiting nutrient within the same reactor configuration.

Both solutions were supplemented with 5 g NaCl L^{-1} to maintain a salinity level equivalent to the average concentration at which the inoculum had been cultivated.

Continuous aeration and mixing of the activated sludge were ensured by an air pump and a mechanical stirrer, except during settling and supernatant withdrawal. Air was supplied to each reactor through a compressor (flow rate=1.8 L min^{-1}) connected to a porous stone with a 6 mm ID silicon tube inserted from the top. An overhead stirrer (Velp Scientifica) was used for mixing (200 rpm). Operational cycles were controlled by a digital timer coordinating stirrer and aeration, synchronized with a programmable logic controller (PLC, Siemens—LOGO! 230RC) managing pumps operations and cycle steps. Temperature was maintained at 25.7 ± 0.2 °C using a recirculating water bath connected to the reactor jacket (Julabo F12-ED). The DO and pH were not controlled but were recorded every minute. DO (S423/C/OPT/T) and pH (S401 DIG/N) probes and the data acquisition system (50Series-4) were supplied by Chemitec Srl.

The operating parameters used in this study are summarized in Table 1, and were selected based on a literature review (Palmeiro-Sánchez et al. 2016b; Montiel-Jarillo et al. 2017; Wang et al. 2020; Argiz et al. 2020, 2021; Matos et al. 2021; Roibás-Rozas et al. 2021; Cruz et al. 2022).

The bacterial community exhibited strong adherence capacity, leading to significant fouling in the bioreactors; therefore, regular detachment was required to keep biomass in suspension and prevent biofilms formation on the reactor walls.

Table 1 Set of operational parameters during the experiment

	N-limiting	P-limiting
Period	I	II
Experimental days	0–314	315–409
SRT (d)	4.4 ± 0.4	4.4 ± 0.4
Hydraulic retention time-HRT-(d)	1.2 ± 0.1	1.2 ± 0.1
Volumetric exchange ratio-VER-(%)	41 ± 4	41 ± 4
OLR (mg O_2 L^{-1} d^{-1})	883 ± 127	776 ± 16
COD:N (gO_2 gN^{-1})	35 ± 6	21 ± 1
COD:P (gO_2 gP^{-1})	142 ± 31	203 ± 11

In this context, meaningful comparison between N- and P-limiting conditions requires the attainment of an operational steady state, defined here as the phase in which steady-state conditions are reached, characterized by a stable feast duration together with constant end-of-famine concentrations of sCOD, NH_4^+-N, and PO_4^{3-}-P, as well as reproducible cycle-to-cycle reactor performance. It should be noted that this operational steady state does not necessarily correspond to a microbial ecology steady state, as no assumption is made that the microbial community has reached full compositional equilibrium.

Analytical methods and data treatment

DO and pH profiles were continuously monitored to assessing the stability of the process. Regular single measurements of ammoniacal N (N-NH_4^+), phosphate (P-PO_4^{3-}) and soluble chemical oxygen demand (sCOD) were performed at the end of the cycle.

To monitor the process in greater detail, single measurements of N-NH_4^+, P-PO_4^{3-} and sCOD were monitored along a selected operating cycle on a monthly basis. Mixed liquor samples were filtered through 0.45 µm membranes and analysed using cuvette kits (Hach Lange, *Germany*): LCK 304 for ammonium, LCK 314 for COD, LCK 349 for phosphate.

PHB, substrate uptake rate (SUR) and total (TSS) and volatile suspended solids (VSS) were determined under N-limiting conditions on experimental day 301 and under P-limiting conditions on experimental day 372. In both cases, single determinations were carried out under conditions considered to represent operational steady state.

PHB was selected as the target polymer for quantification as it is typically the dominant storage polymer produced by MMCs under the operating conditions applied, particularly when acetate is the main carbon source (Dias et al. 2008). Although the presence of propionate in the feed could potentially lead to the formation of

hydroxyvalerate (HV), its contribution was considered secondary in this system and was not specifically quantified. Therefore, the reported polymer data reflect PHB accumulation only and do not account for possible HV contributions to total PHA content. This may lead to a slight underestimation of the total PHA accumulated in the system.

PHB was quantified as crotonic acid by HPLC using the following procedure. Sludge samples were collected from the reactor at the end of the growth phase and centrifuged in a Sorvall Super T21 centrifuge at 12,000 rpm for 3 min. After centrifugation, the biomass pellet was stored at − 20 °C and later subjected to acidic digestion by adding 1 mL of pure sulphuric acid and incubating the solution at 105 °C for 30 min to convert PHB to crotonic acid. Crotonic acid was eluted from a Synergy-Hydro-RP C-18 column (205 × 4.6 mm i.d., Phenomenex, USA) using an HPLC-Thermo Finnigan-Spectra System 6000LP, USA, and detected by ultraviolet absorption at 214 nm. The mobile phase consisted of 15% (v/v) acetonitrile and 0.1% (v/v) H_3PO_4 in aqueous solution, with a flow rate of 1.0 mL/min. Pure PHB (Biomer, Krailling, Germany) converted to crotonic acid was used to generate the calibration curve. Duplicate spot analysis indicated an analytical variability of approximately 10%, reflecting the degree of variation observed between repeated measurements of the same sample.

The SUR [mg L^{-1} h^{-1}] was computed as the slope of the line approximating the descending profile of the sCOD measurements, representing the uptake rate of the carbon source during the feast ($-\Delta$sCOD t_{feast}^{-1}) where ΔsCOD is the change in soluble COD concentration [mg L^{-1}] and t_{feast} is the corresponding time interval [h]. In accordance with the Standard Methods (APHA 1998), mixed liquor was sampled from the reactor to determine TSS and VSS, with measurements performed in triplicate. The specific SUR (SSUR) is the SUR normalised for average VSS concentration (Eq. 1).

The maximum PHB content (PHB_{max}) was calculated as the percentage of PHB in VSS, where VSS represents the sum of PHA and active biomass (Eq. 2). Additional performance indicators were evaluated to assess process performance, including PHB storage yield and PHB volumetric productivity. The PHB storage yield (Y_{PHB}) was defined as the ratio between PHB formed and substrate uptake (ΔCOD) (Eq. 3) as reported by Moretto et al. (2020). PHB volumetric productivity was calculated as the daily PHB mass leaving the reactor, following Cabrera et al. (2021), assuming biomass withdrawal at the end of the feast phase (Eq. 4). PHB at the end of the famine phase was not directly measured and was assumed to be negligible based on the expected complete substrate consumption under starvation conditions. While this assumption is consistent with the operating conditions of the process, it represents a limitation of the study and should be considered when interpreting yield calculations and mass balances.

$$\text{Specific SUR (SSUR)} \quad \text{SUR VSS}^{-1} \tag{1}$$

$$\text{Max PHB content } \left(\text{PHB}_{max}\right) \quad \text{PHB VSS}^{-1} \tag{2}$$

$$\text{PHB storage yield } \left(\text{Y}_{PHB}\right) \quad \text{PHB } \Delta\text{sCOD}^{-1} \tag{3}$$

$$\text{PHB volumetric productivity} \quad 2 \cdot \text{PHB} \cdot \text{VSS} \tag{4}$$

DNA extraction, 16S amplification and sequencing

Samples of the mixed liquor were collected over time, centrifuged and the pellet stored at − 20 °C Thirty-two samples were collected overall, of which 10 were associated with the N-limitation period (including the inoculum) and 22 with the P-limitation period.

To assess the amount of stochastic variation in the data and the robustness of the processing, technical replicates were sequenced for both the inoculum (day 1) and the sample collected on day 70. Briefly, for each sample, total DNA was purified, the V3-V4 region of the 16S rRNA gene was amplified, and the resulting amplicons were sequenced. In detail, the total DNA was extracted from 200 mg of each sample using the DNeasy PowerSoil Pro kit (Qiagen, Hilden, Germany). Cell lysis was performed through 6 cycles of bead-beating for 30 s at a rate of 5 m/s using a Savant FastPrep 120, allowing the sample to cool to room temperature for 1 min every two cycles. The remaining steps of the DNA extraction were conducted according to the manufacturer's instructions. All DNA extraction steps were performed under sterile conditions, and an extraction blank was co-processed to assess potential contamination. The blank yielded no detectable DNA by NanoDrop as assessed by NanoDrop spectrophotometry, confirming the absence of detectable contamination in the procedure. Afterwards, 12.5 ng of DNA were used as input in 25 polymerase chain reaction -PCR- cycles with a final volume of 20 µL, according to Illumina's 16S library preparation protocol, using the Platinum SuperFi II kit (Invitrogen, Massachusetts, America). In particular, the DNA template encompassing the region V3-V4 of the 16S rRNA was amplified using the primers Pro341FB (CCTACGGGNBGCWSCAG) and 805R (GACTACNVGGGTWTCTAATCC), given the improved coverage of PRO341FB for environmental microbial communities (Mazzoli et al. 2020) than Pro341F proposed in the default Illumina protocol.

The quality and the quantity of the amplicons obtained were assessed by measuring the signals intensities on electrophoresis on 1% agarose gel stained with ethidium

bromide. Finally, amplicons from each sample were normalised to the same concentration and sent to BMR Genomics S.r.l. (Padova, Italy) where it was sequenced in paired-end mode (2 × 300 cycles) on the Illumina MiSeq platform.

Sequenced DNA processing

Demultiplexed sequence reads were processed using QIIME2 (Bolyen et al. 2019). Sequencing primers and reads without primers were removed using the Cutadapt tool (Martin 2011). In order, DADA2 (Callahan et al. 2016) was used to perform trimming of low-quality regions (forward reads truncated at 276 bp and reverse reads at 196 bp), overall quality filtering, merging of paired reads and removal of chimeras, resulting in generations of amplicon sequence variants (ASVs). ASVs taxonomic assignments were performed using the Scikit-learn naive Bayes multinomial classifier re-trained on the SILVA SSU database (Release 138) V3-V4 hypervariable database (Quast et al. 2013). All ASVs associated to genera with the highest relative abundance in samples below the 0.005% cut-off were discarded to minimise contaminants and sequencing errors and to improve statistical inference (Bokulich et al. 2013; Cao et al. 2021). In addition, ASVs identified as mitochondria according to SILVA were also discarded. Finally, reads not identified at the phylum level were discarded as potential eukaryotic off-target contaminants resulting from primer mismatches to similar eukaryotic sequences (Di Gloria et al. 2025). Additional details on read processing and associated scripts are available at [*https://github.com/LeandroD94/Papers/tree/main/2024_PHA_microbiota_N_P_condition*].

Taxonomic and statistical analyses of microbial data

The statistical analyses on bacterial communities were performed in R 4.3 with the help of the packages phyloseq 1.44.0 (McMurdie and Holmes 2013), vegan 2.6–4 (Oksanen 2024), DESeq2 1.40.1 (Love et al. 2014), microbiome 1.24.0 (Lahti and Shetty 2017) and other packages satisfying their dependencies. Data visualization was performed using the packages ggplot2 3.4.2, ggh4 × 0.2.4 and ggpubr 0.6.0. A saturation analysis of the ASVs was performed on each sample using the rarecurve function (step 100 reads), further processed to highlight saturated samples (arbitrarily defined as saturated samples with a final slope of the rarefaction curve with an increase in the number of ASVs per reads < $1e^{-5}$).

Microbial community composition was first described in terms of overall structure, focusing on the most abundant phyla and genera. These were identified based on highest average relative abundance, calculated using only samples collected during the second half of N- and P-limiting periods, in order to characterize microbial communities at later stages of development under each condition.

Alpha-diversity was estimated at genus level through observed richness, Shannon indices and Pielou's evenness indices. Pielou's evenness index was calculated using the formula E = S/log(R), where S is the Shannon diversity index and R is the observed richness in the sample.

Beta diversity was evaluated through Principal Coordinate Analyses (PCoAs) computed at genus level using the Hellinger distance (euclidean distance on Hellinger transformed abundances) given the sparse and compositional properties characterising the microbiota sequencing data (Legendre 2012; Quinn et al. 2019).

The variation of genera abundances over time was tested using Spearman's method on counts transformed into Centered Log Ratio (CLR), thereby reducing false positives due to compositional effects (Quinn et al. 2019). Technical replicates and genera featured as traces (i.e., <0.01% relative abundance and present in only a few samples) were excluded from the correlation analysis. Results with p-values below 0.05 after Benjamini–Hochberg correction for multiple testing were considered statistically significant.

Genera potentially capable of PHA biosynthesis were outlined after an accurate literature review. Thus, a total of 60 genera associated with PHA biosynthesis (listed with their references in Table S1 of the supplementary material) were searched in the analysed data. Any taxonomic synonymies were solved by searching each name in the LPSN (List of Prokaryotic names with Standing in Nomenclature) (Parte et al. 2020).

Additional details on microbial profiling and statistical analyses are publicly available at [*https://github.com/LeandroD94/Papers/tree/main/2024_PHA_microbiota_N_P_condition*].

Results and discussion

SBR enrichment under different limiting nutrients

The evolution over time of the SBR performance subjected to an UF strategy, first under N-limiting and then P-limiting conditions, was evaluated. In particular, the PHB accumulation performance of biomass enriched under conditions of N and P limitation was compared once it had reached its steady state. The steady-state period was identified by examining the feast duration [h] over time. The feast duration was calculated according to the oxygen concentration profile as the time span between the end of the feeding phase and the time in which the oxygen concentration started rising due to C depletion. In Fig. 2, the feast duration over all the experiment is plotted: two transient phases emerged as a result of the shifts in enrichment strategies, one after

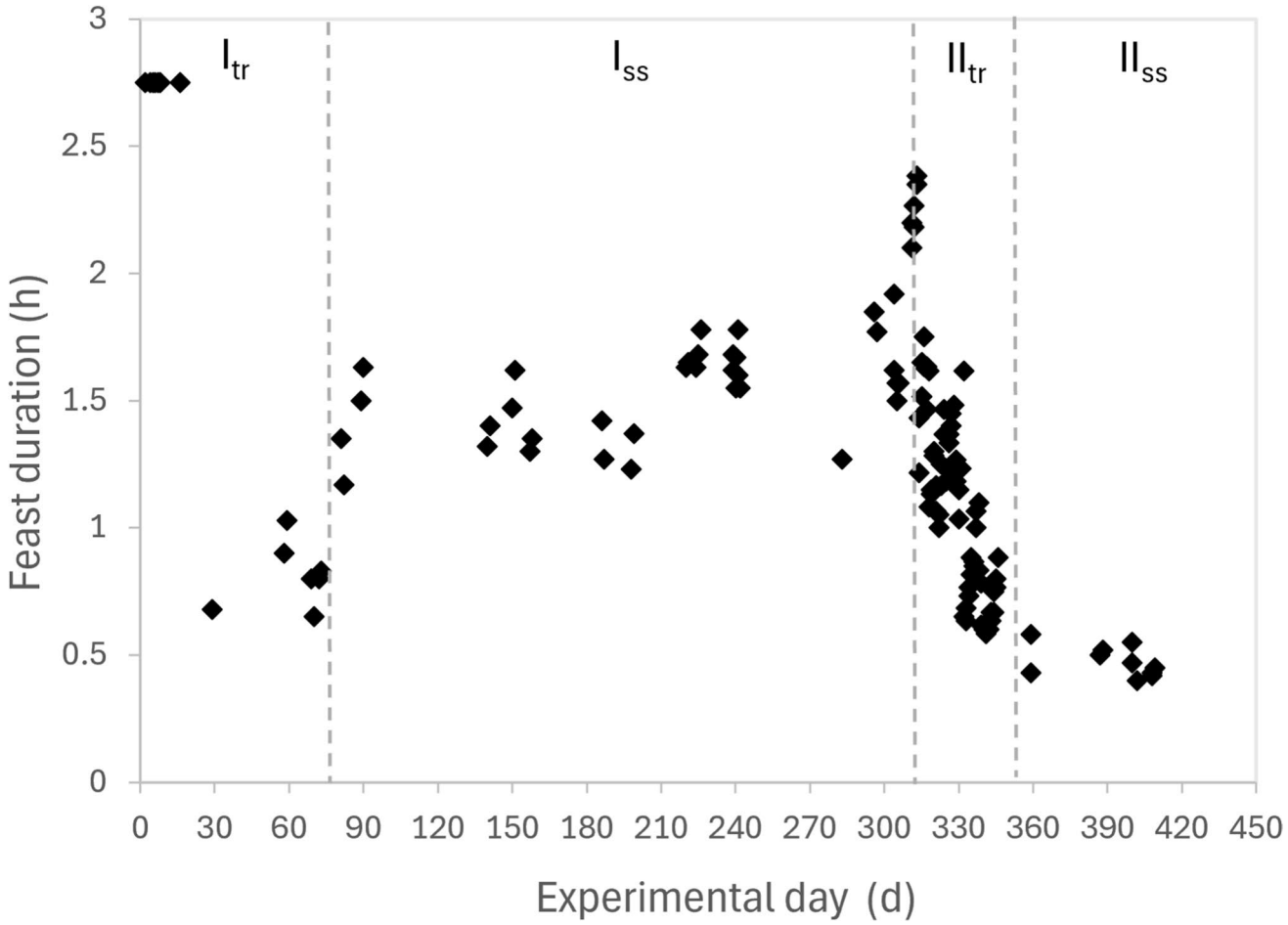


Fig. 2 Feast duration along the experimental periods

Table 2 Overall outcomes throughout the experimental periods measured at the end of the cycle

		N-limiting		P-limiting	
Variable/period		I_{TR}	I_{SS}	II_{TR}	II_{SS}
Experimental day		1–80	81–314	315–358	359–409
sCOD	(mg L^{-1})	121 ± 19	82 ± 34	60 ± 20	60 ± 12
$N_NH_4^+$	(mg L^{-1})	5 ± 8	0.1 ± 0.1	10 ± 3	13 ± 2
$P_PO_4^{3-}$	(mg L^{-1})	6 ± 3	3 ± 2	0.09 ± 0.2	<0.05
TSS	(g L^{-1})	1.7 ± 0.7	0.8 ± 0.4	0.7 ± 0.2	0.8 ± 0.5

Table 3 Main results comparison between N (period I_4) and P (period II-steady state) limiting conditions

Variable/period	N-limiting	P-limiting
Experimental day	301	372
VSS (mg L^{-1})	633±65	405±11
SUR (mg sCOD L^{-1} h^{-1})	152	697
SSUR (h^{-1})	0.2	1.7
PHB (%)	29±5	9±1
Y_{PHB}	0.51	0.10
PHB productivity (mg PHB L^{-1} d^{-1})	367	73

inoculation under N-limiting conditions (I_{TR}) and the other after switching to P-limiting conditions (II_{TR}), along with two steady-state periods (I_{SS} and II_{SS}).

Table 2 shows the concentrations of sCOD, $N\text{-}NH_4^+$, $P\text{-}PO_4^{3-}$ and TSS measured at the end of the cycle throughout the experimental periods, providing an indication of the magnitude and stability of these parameters in the different phases of the experiment (I_{TR}, I_{SS}, II_{TR}, II_{SS}).

Table 3 shows the main results obtained from the cycle analyses at steady-state conditions during period I_{SS} (day 301) and II_{SS} (day 372). From the analyses performed, a different behaviour was observed in the SBR. The PHB storage at the end of the accumulation phase was higher (29%) under N-limiting conditions than PHB accumulation under P-limiting conditions (9%). Another noticeable difference concerns the SUR and SSUR, also resulting in a different

duration of the feast phase (Fig. 2): 1.5 h under N-limiting condition and 0.5 h under P-limiting condition.

Therefore, N-limiting conditions ensure a higher PHB accumulation (more than three times) and lower SUR (− 80%) compared to that under P-limiting conditions.

Complementary, the typical pattern of the main parameters (sCOD, N-NH_4^+, P-PO_4^{3-}, DO, pH) throughout a standard SBR cycle is depicted in Fig. 3, under N-limiting conditions on day 226 (Fig. 3A), and under P-limiting conditions on day 408 (Fig. 3B).

Biomass activity was clearly reflected in variations in both DO and pH. In both scenarios the consumption of the C source coincided with a pronounced DO decrease during the accumulation phase and a less pronounced decrease during the growth period. The pH showed an increase just after substrate feeding during the external substrate uptake, followed by a prompt decrease once DO returns to saturation and substrate removal ceased. Throughout the growth phase, the pH continued to decrease until reaching a minimum, after which it began to rise again, likely occurring when the rate of CO_2 stripping exceeded the rate of CO_2 production associated with growth. These pH changes, while distinct, occurred within a relatively narrow range from 8.3 to 8.9.

With respect to the DO profile, the most relevant difference is that under P-limiting conditions, oxygen consumption associated with growth was more evenly distributed throughout the cycle. Regarding pH, a sharper decrease was observed after the feast phase under P-limiting conditions (Fig. 3). Both patterns suggest growth signals occurring outside the designated growth period.

A further, albeit small, yet potentially significant difference was observed in the sCOD profile. A temporary increase in sCOD followed by its rapid uptake (Fig. 3A) was observed under N-limiting conditions at the beginning of the growth phase. Such sCOD behaviour was hypothesized to correspond to a release and subsequently reabsorption of an organic substrate, which may correspond to Soluble Microbial Products (SMPs), defined as complex organic compounds originating from substrate metabolism and biomass decay (Kunacheva and Stuckey 2014). Such behaviour was not observed under P-limiting conditions (Fig. 3B) possibly indicating that growth under P-limiting conditions is not restricted to the early part of the growth phase, as they are under N-limiting conditions. Recent studies, such as the one on mung bean fermentation by *Aspergillus niger* shows that untargeted metabolomics can characterize SMPs beyond bulk COD, revealing them as dynamic, stage-dependent metabolite mixtures linked to specific metabolic pathways. In line with these findings, in N-limited systems SMPs may therefore interpretated not merely as metabolic byproducts, but as potential functional indicators of shifts in metabolic strategy and resource allocation (Lang et al. 2025).

Importantly, it is assumed that the levels of N and P decreased during the growth phase in the UF, with the limiting nutrient being entirely consumed during this phase, thereby constraining growth in the subsequent accumulation phase due to its unavailability. It was observed that under both N- and P-limiting conditions, the limiting nutrient was depleted during the growth phase (Fig. 3). Nevertheless, under P-limiting conditions, ammonium uptake is observed during the accumulation phase despite the absence of P (less than 0.05 mg P/L), suggesting microbial growth during the accumulation phase (Fig. 3B).

Taxonomic analysis of the shifting microbial community

The bacterial community evolution subjected to an UF strategy, first under N-limiting and then P-limiting conditions, was evaluated over time. Sequencing yielded a total of 3,348,556 reads, of which 1,880,647 (56.16%) passed quality filters (Figure S1). After filtering, 43 genera were discarded, each of which was scarcely present in few samples as trace amount, thus having minimal impact on further reducing the amount of reads available for analysis (1,880,501 retained reads). The filtered reads were identified as arising from 486 genera, of which 431 were taxonomically classified at the genus level by the classifier. Each specimen proved to be ecologically saturated according to the saturation analysis computed on the retained reads, with the exception of the sample collected on experimental day 373, which featured a saturation curve far from reaching the plateau (Figure S2). Accordingly, this sample has been discarded from the analysis. Negligible variation among abundant taxa between technical replicates of the inoculum DNA sequencing was observed (Figure S3). On the other hand, the greater sequencing depth achieved in one replicate allowed the detection of a slightly higher number of genera in it, although only at trace abundance (i.e., mostly below 0.001%).

The most abundant phyla in the inoculum were Actinobacteriota (33.7%), Proteobacteria (32.8%), Chloroflexi (13.6%), Bacteroidota (10.2%) and Planctomycetota (3.1%) while the most abundant genera were the genus *67–14* of Solirubrobacterales order (20.9%), *Defluvicoccus* (9.2%), *JG30-KF-CM45* (5.5%), *AKYG1722* (4.6%) and *Hyphomicrobium* (3.5%) (Figure S3).

Under N-limiting condition, a rapid community shift was observed. Within approximately a month, thriving of genera potentially involved in PHA biosynthesis was observed. At phylum level, a decrease in Actinobacteriota, Chloroflexi, and Planctomycetota was observed, while Proteobacteria (66.9%) and Bacteroidota (16.4%) became dominant, together with minor contributions from Verrucomicrobiota, Firmicutes, and Planctomycetota. At genus level, the

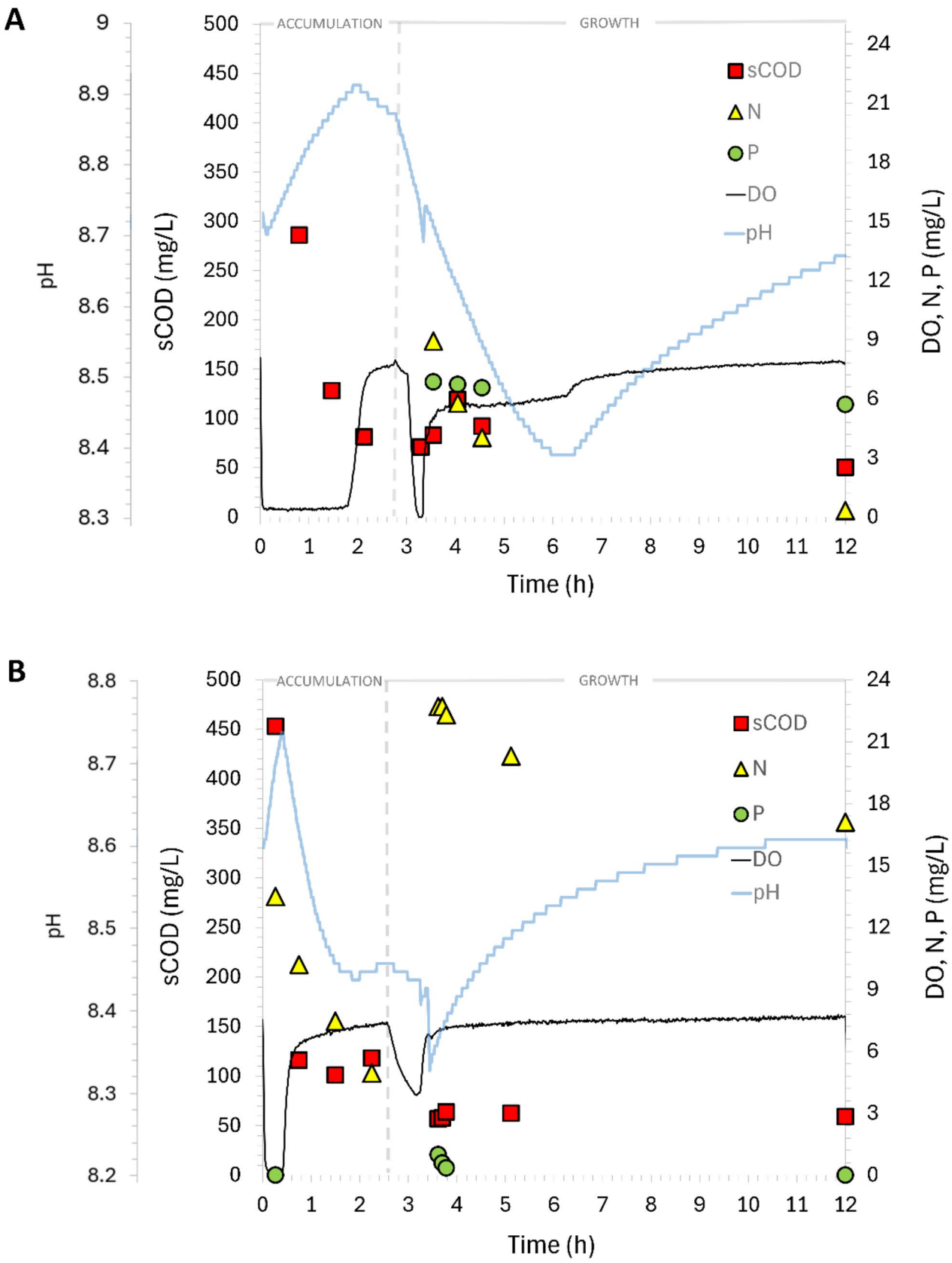


Fig. 3 Profiles of the main parameters during a typical cycle under N (**A**) and P (**B**) limiting conditions

community became dominated by *Neomegalonema* (29.1%), *Paracoccus* (11.5%), *Flavobacterium* (7.4%), *Azoarcus* (5.2%), *Stappia* (2.8%), *Planktosalinus* (1.9%), *Azonexus* (1.4%), *Thauera* (1.4%), *Gemmobacter* (1.2%), and *Prosthecobacter* (1.2%). Refer to Figure S4 for further details.

Microscopy revealed that the biomass cultivated under N-limiting conditions was rich in filamentous bacteria and protozoa (Figure S5).

Under P-limiting conditions, the overall phylum-level structure remained similar, except for small variation in relative abundances, whereas more substantial differences were found at the genus level. Specifically, under P-limiting phase, the most abundant phyla were Proteobacteria (75.9%), Bacteroidota (19.4%), Firmicutes (1.2%), Verrucomicrobiota (1.6%) and Planctomycetota (0.7%) while the most abundant genera were *Paracoccus* (34.7%), *Neomegalonema* (24.8%), *Planktosalinus* (15.3%), *Thauera* (11.4%), *Azoarcus* (3.1%), *Subsaxibacter* (1.5%), *Prosthecobacter* (1.0%), *Fusibacter* (0.7%), *SM1A02* (0.4%) and *DEV007* (0.3%). Refer to Figure S6 for further details.

The overall gradual change throughout the days of the experiment can be observed in Fig. 4.

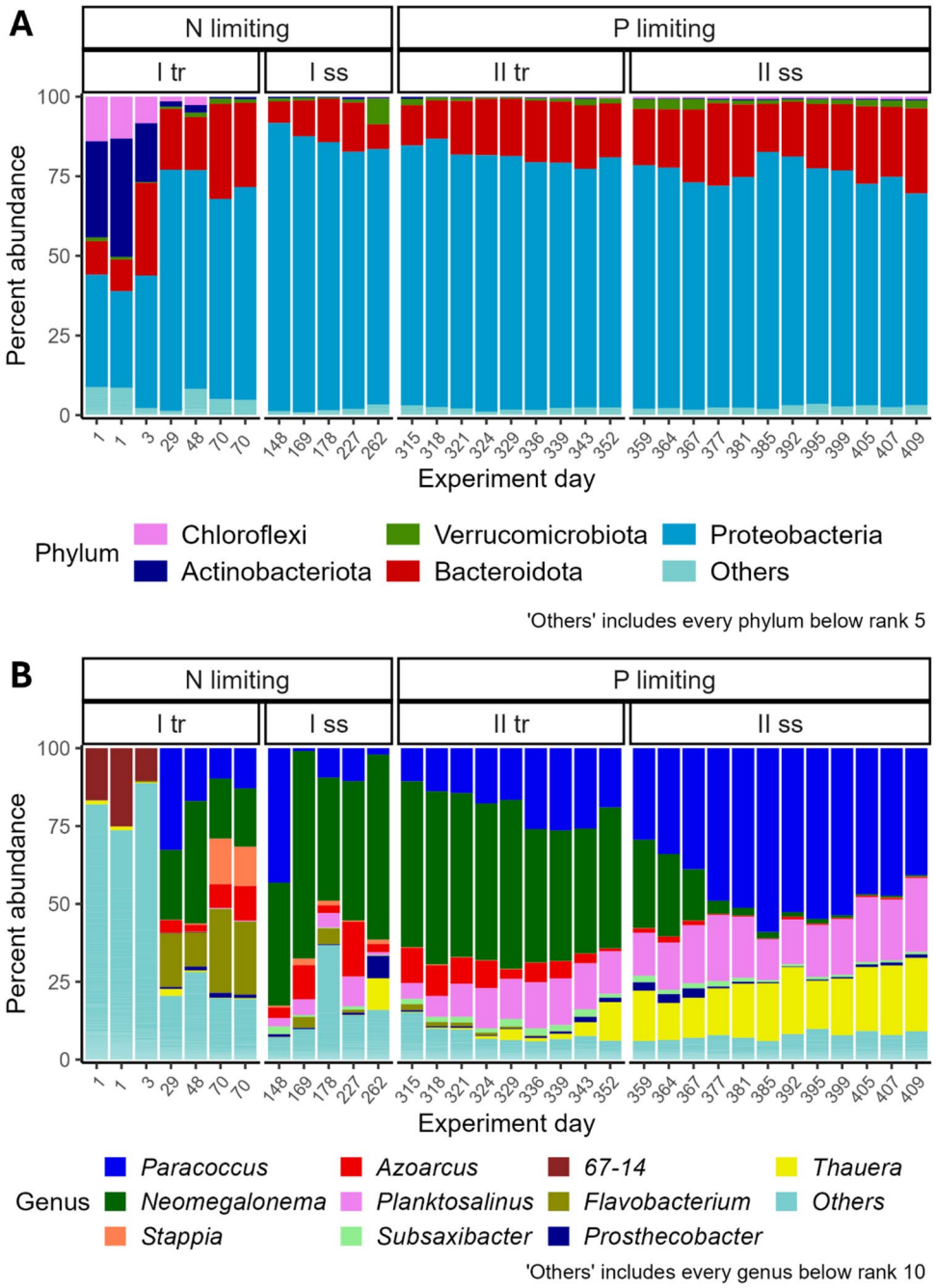


Fig. 4 Microbial composition. Stacked bar plot of the relative abundances of five most abundant phyla (**A**) and ten most abundant genera (**B**)

The apparent increase of *Neomegalonema* and *Azoarcus* under N-limiting condition was not statistically significant, according to Spearman's correlation, whereas the abundances of an unidentified genus of Flavobacteriales order and three uncultured genera of Cyclobacteriaceae, Blastocatellaceae and Paracaedibacteraceae families were significantly increased during such condition (Figure S7 and Table S2). Whereas the noticeable decreases in the abundances of *Neomegalonema* and *Azoarcus* and the rise of *Paracoccus, the* genus *SM1A02* of Planctomycetota phylum and *Thauera* under P-limiting condition were reported as significant by the correlation analysis (Figure S8 and Table S3).

The community underwent marked selection relative to the inoculum, leading to a reduction in observed genus richness and abundances evenness throughout the experiment, resulting in about one hundred distinct genera being identified in each sample during both N- and P-limitation periods (Fig. 5A). The continuous and gradual shift of the whole microbial communities along the experiment is well represented by their PCoA representation (Fig. 5B). While a minimum distance is exhibited by the technical replicates (sample relative to days 1 and 70), both N- limiting (Fig. 5) and P- limiting (Fig. 5) conditions appear to act as strong drivers of community composition. As expected, time flow is a major structuring factor especially under P-limiting conditions, which alone PC1 explains 86.8% of data variability (Fig. 5D). A substantial community shift was observed during the first 30 days, reflecting the ecological selection of different dominant taxa and the reduction in alpha diversity described above. Samples under N-limiting conditions began clustering around day 148 while P- limiting conditions samples clustered around day 377 (Fig. 5), i.e. 62 days after the transition to P-limiting conditions, representing the time required for microbial community to reach an overall stability. This difference should be interpreted considering that the P-limiting phase started from an already enriched PHA-accumulating community, whereas N limitation was applied to a raw activated sludge inoculum.

In both cases, the first microbial steady state is established later than the operational steady state (Figs. 2 and 5). This highlights that process stability inferred from operational parameters alone may not fully capture the underlying microbial dynamics.

A total of 27 genera previously reported in the literature as potentially associated with PHA accumulation were detected. Among these, *Neomegalonema*, *Paracoccus*, *Azoarcus* and *Thauera* were predominant (Fig. 6). As expected, PHA-related genera were poorly represented in the inoculum but started to thrive from day 29 onwards, reaching more than 60% of total relative abundance in each sample (Fig. 6). Notably, the PHA related genera *Hyphomicrobium* and *Defluviicoccus*, initially present in the inoculum, were detected only at trace levels during the first days of experimentation but absent in mature communities.

Traces of *Bdellovibrio* (~0.1%) was detected across most sample, including the inoculum. This result may be interpreted as an overall positive outcome, since this genus is known to contain predators of PHA producers, potentially leading to suboptimal PHA yields and system collapse (Clagnan and Adani 2023). Finally, four archaea genera are scarcely present among the samples, namely *Methanobrevibacter, Methanolobus, genus SCGC_AAA286-E23* and *Methanosaeta,* but with low relative abundances (0.005–0.1%).

Assessment of PHA accumulation performance and tentative interpretations

From an accumulation perspective (PHB content, Y_{PHB}, and volumetric productivity), higher performance was observed under N limitation rather than P limitation. Overall, the results suggest that biomass growth was not fully suppressed under P-limiting conditions during the accumulation phase, possibly contributing to lower storage performance.

In fact, it can be observed that under N-limiting conditions the absence of N (less than 0.2 mg L^{-1}) resulted in no P removal. Conversely, under P-limiting conditions, the absence of P (less than 0.05 mg P L^{-1}) did not prevent N removal, which occurred in both the accumulation and growth phases (Fig. 3B).

Mass balances of sCOD, N, and P during representative cycles showed a P:N ratio of 0.4 under N limitation, dropping to 0.2 under P limitation, may be due either to selection of biomass with lower P content or P sourced from the environment, possibly released by biomass decay as orthophosphate or through accumulation/release cycles. Organisms with higher P affinity or intracellular storage capacity might have been favoured. P accumulation is not necessarily linked to P-accumulating organisms (PAOs), which were only slightly favoured and not detected microbiologically. The amount of accumulated P was not directly measured in this study. In P-limiting systems, iron and other trace metals may significantly influence P fate by promoting adsorption and co-precipitation onto Fe(III) minerals, thereby affecting its availability and immobilization (Chen et al. 2025). Therefore, future work would benefit from including measurements of iron speciation and dynamics, as well as P accumulation.

Literature reports show contrasting outcomes depending on reactor configuration and nutrient regime. It should be noted that comparisons with previous studies must be interpreted in light of the sequential single-reactor design adopted here, where nutrient effects are not fully separable from temporal adaptation and cumulative selection processes.

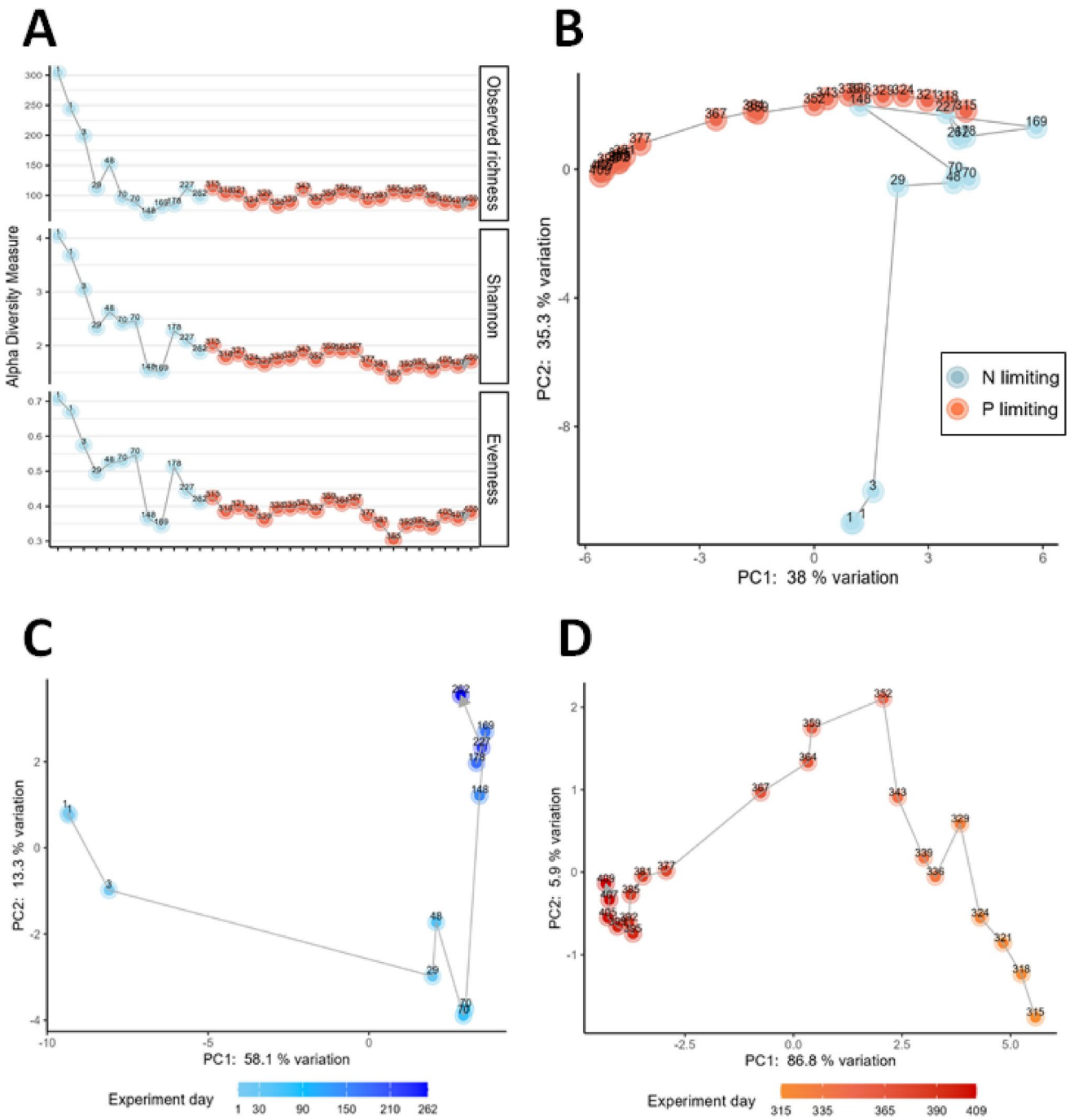


Fig. 5 Alpha diversity indices (**A**) and Principal coordinate analysis (PCoA) of samples along the experiment (**B**), under N-limiting (**C**) and P-limiting (**D**) conditions. The experiment day is displayed as number on each point and also as colour gradient in the plots C and D

Wen et al. (2010) observed higher PHB accumulation under N limitation compared to P limitation in parallel SBR systems, consistent with the trends observed here, and attributed this to reduced anabolic activity under N limitation: PHA accumulation peaked at 59% under N limitation (C:N = 125) versus 14% under P limitation (C:P = 250). They suggested that N limitation impaired protein synthesis, shifting metabolism toward PHA storage, whereas P limitation still supported cell growth and anabolism. They also observed filamentous bulking under N-limiting conditions, in agreement with the microscopic observations in this study.

Alternatively, Brison et al. (2022) reported efficient selection of PHA-storing communities under P limitation at high COD:P ratios in a CSTR system. They achieved >90%

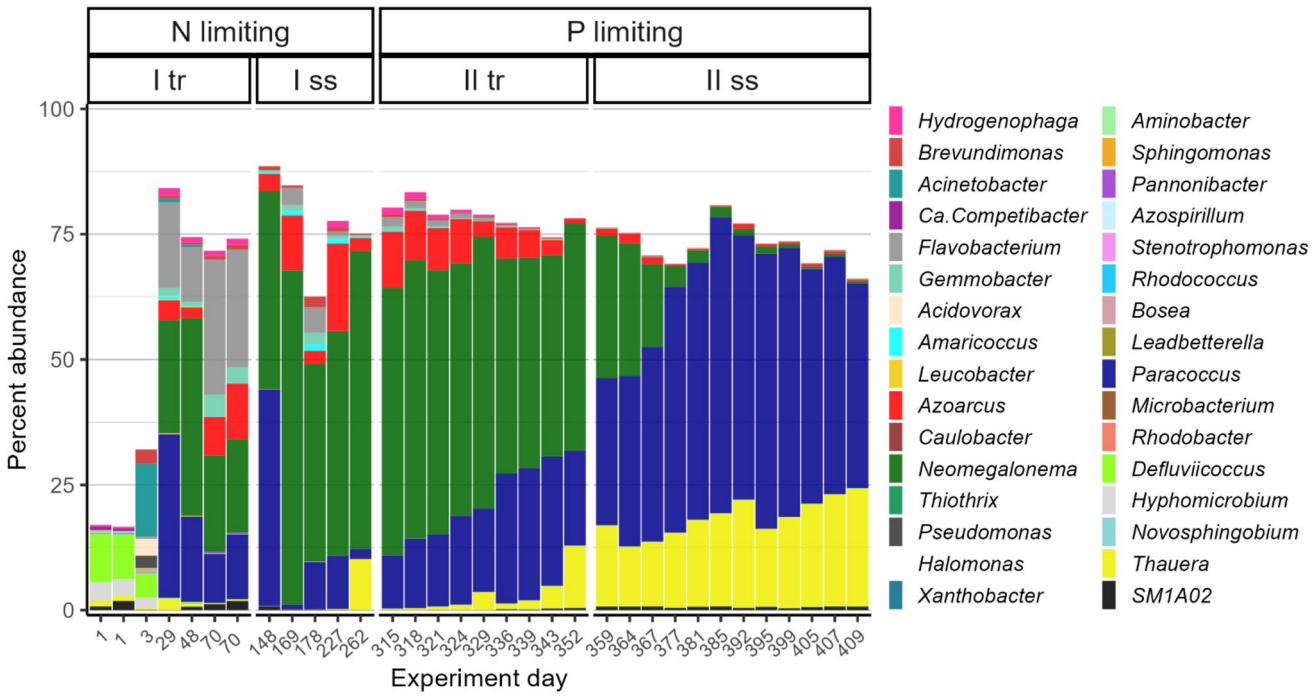


Fig. 6 Bar plot of the percent abundances of PHA accumulating genera featured in the samples

PHA accumulators at high influent COD:P (800 gO_2 gP^{-1}). Authors attributed this fact to heterotrophs' dependence on P-rich ribosomes and RNAs for growth, whereas nutrient uptake proteins require no P.

Similarly, Korkakaki et al. (2017) reported that PHA was stored at high C:P ratios (300 Cmol mol^{-1}), whereas rapid polyphosphate accumulation occurred at low C:P ratios (150 Cmol mol^{-1}). Authors also suggested that in continuous operation substrate affinity drives bacterial competition, while in SBR the uptake rate of the most limiting substrate is decisive.

Overall, our findings are in line with Stouten (2021), who reported ammonium assimilation during the accumulation phase under P-limiting conditions (C:P=200–300 mol mol^{-1}).

These observations highlight that the extent of nutrient limitation is a key factor. Gaining this understanding requires knowledge of the biomass C:N:P stoichiometric ratio, which remains largely unknown, particularly for P, whose content varies across microbial taxa (Franklin et al. 2011). Moreover, these ratios can vary over time, as microorganisms can adjust their cellular C:P ratio to ensure cell division (Stouten 2021; Brison et al. 2022). Under P-limited conditions, microorganisms regulate nutrient uptake and allocation to maintain cellular stoichiometry, enhancing P acquisition and retention rather than allowing intracellular depletion. Compared with N limitation, microbial communities may sustain growth under low P by improving P-use efficiency and conserving internal pools. A larger fraction of C is directed toward maintenance and nutrient scavenging rather than storage, which may explain the observed reduction in PHB accumulation as a potential trade-off between energy-demanding uptake processes and C storage metabolism (Liu et al. 2023). The uncoupling between ammonium uptake and biomass growth under P limitation can be interpreted by analogy with nutrient-constrained fermentation systems, where environmental stress leads to incomplete metabolic pathways and byproduct accumulation. Similarly, under P limitation, biomass synthesis may be restricted due to the central role of P in ATP production, nucleic acid synthesis, and membrane formation, while ammonium uptake can still proceed. As a result, nutrient assimilation becomes partially decoupled from growth, with C and energy fluxes redirected toward maintenance, respiration, or nutrients storage pathways (Zhou et al. 2024).

Understanding microbial dynamics during selection processes: causes and implications

The present work tracked microbial community evolution under two sequential conditions (N- and P-limiting conditions). Starting from the inoculum, significant compositional shifts were observed ("Taxonomic analysis of the shifting microbial community" section), with Proteobacteria rapidly dominating under both conditions (Fig. 4A). The dataset was largely composed of *Neomegalonema*, *Paracoccus*,

Flavobacterium, *Azoarcus*, and *Thauera*, several of which have been previously reported in PHA-accumulating MMCs (Coats et al. 2016; Wang et al. 2017; Correa-Galeote et al. 2022; Carvalho et al. 2022; Zhang et al. 2024). A shift in bacterial community composition at the genus level was observed following the transition from N to P limitation. A similar pattern was reported by Stouten (2021); although involving different bacterial genera, the microbial community changed under N- or P-limiting conditions.

One of the most evident trends was the decrease of *Neomegalonema* under P-limiting conditions. *Neomegalonema*, also referred to as *Meganema* by (Thomsen et al. 2006), is recognized for its capacity to accumulate significant amounts of PHA and is known to cause bulking issues in WWTPs due to its filamentous morphology. Currently, *Neomegalonema perideroedes* is the only known and morphologically, genetically, and ecologically described species of this genus (Cruz et al. 2022; Clagnan and Adani 2023). This genus exhibits high substrate affinity and exceptionally high uptake rates, comparable to or exceeding those of floc-forming bacteria. Notably, *Neomegalonema* consumes soluble short-chain substrates without requiring prior hydrolysis (Kragelund et al. 2005). In pure culture, they form off-white cohesive colonies that are difficult to separate (McIlroy et al. 2015), consistent with the observed cohesive biofilm in activated sludge. *Neomegalonema* can uptake acetate, propionate, and butyrate, showing a preference for acetate and propionate (Wang et al. 2020). *N. perideroedes* possesses a gene coding for a low-affinity phosphate transporter (McIlroy et al. 2015). Accordingly, under P-limiting conditions, microbial competition likely hinges on P affinity, potentially leading to the outcompetition of *Neomegalonema*, assuming that the most abundant species within this genus was *N. perideroedes*. Notably, the limited taxonomic resolution of 16S rRNA gene amplicon sequencing prevents the confirmation of this inference. Alternatively, the reduction of this genus under P limitation may be associated with altered process conditions, including differences in substrate uptake rates (SUR), which create significantly different conditions during the accumulation phase under the two different limitations (N and P). Although DO drops near zero under both N- and P-limitation during the accumulation phase, creating a microaerophilic environment in the SBR, higher SUR in P-limitation lead to a quicker return to aerobic conditions, whereas under N-limitation, the microaerophilic phase lasts longer. This difference may explain the presence of filamentous bacteria under N-limitation and their disappearance under P-limitation; their presence may be linked more to DO limitation than directly to N- or P-limitation. Consistently, the presence of methanogens was observed only under N-limiting conditions, indicating more anaerobic conditions under N limitation than under P limitation. However, these interpretations remain hypothetical, as direct physiological confirmation is not available.

Another interesting result was the increase of *Thauera* under P-limiting conditions. *Thauera* can synthesize 3-hydroxybutyrate-*co*−3-hydroxyvalerate (PHBV) with different HV unit content by using different ratios of acetic and propionic acids (Andreolli et al. 2022; Carvalho et al. 2022). In the present study, PHB was considered the main product, as acetate represented the dominant carbon source (80%), while propionate (20%) was not further resolved in terms of potential HV formation, which remains outside the scope of this work.

Other taxa identified through correlation analysis, including *Flavobacteriales*, *Cyclobacteriaceae*, *Paracaedibacteraceae*, *SM1A02* (Planctomycetota), and *DEV007* (Verrucomicrobiota), showed condition-dependent trends. However, these associations should be interpreted cautiously, as they reflect statistical correlations rather than demonstrated functional roles.

To our knowledge, the genus *SM1A02* has been reported in only two previous studies as PHA accumulating bacteria (Cui et al. 2016; Wen et al. 2024), has good nitrification performance and represents a putative novel anammox bacterium (Tian et al. 2017). Since *SM1A02* belongs to the Planctomycetota phylum, its reliable detection was facilitated by the use of primer PRO341FB (Mazzoli et al. 2020), which effectively amplifies the V3-V4 region of the 16S rRNA gene in Planctomycetota, reducing the risk of underrepresentation.

Taxonomic differences may have played in shaping accumulation performance, but the differences can be interpreted also in terms of system functionality. In this context, studies on engineered living materials have shown that nutrient distribution strongly influences microbial growth and community organization. Using 3D bioprinting approaches, mainly based on filamentous fungi, it has been demonstrated that low nutrient availability promotes an explorative growth strategy characterized by rapid extension, whereas nutrient-rich conditions favour a more compact, biomass-oriented strategy. These findings indicate that microbial structure and function are primarily driven by nutrient availability rather than taxonomy alone (Teoh et al. 2024).

Valorisation of saline effluents through PHA production

Saline wastewater is increasingly generated by industries such as pharmaceuticals, petrochemicals, and food processing. High salinity exerts a strong selective pressure on microbial communities, as elevated NaCl concentrations induce osmotic stress, cellular dehydration, enzyme inactivation, and inhibit growth and metabolic activity in non-adapted

microorganisms. To cope with these conditions, salt-tolerant microorganisms may adopt multiple strategies, including the synthesis of compatible organic solutes (e.g. betaine and trehalose), extracellular polymeric substances (EPS) production, and intracellular PHA accumulation.

From an applied perspective, the use of saline waste streams in combination with MMCs represents a potentially interesting strategy for coupling wastewater treatment with biopolymer production (Wen et al. 2024).

In this study, activated sludge from tannery wastewater was successfully used as inoculum, and enrichment under the applied UF strategy resulted in a stable PHA-producing community capable of operating under 5 g NaCl L^{-1}. These results demonstrate the feasibility of maintaining PHA production under mild saline conditions.

However, the physiological mechanisms underlying salt tolerance in the enriched community were not directly investigated in this work. Wen et al. (2024) reported that genera such as *Thauera*, *Paracoccus*, *Prosthecobacter*, and *SM1A02* act as PHA producers and exhibit strong positive associations with glycine and betaine biosynthesis and transport genes suggesting that these microorganisms preferentially synthesize compatible solutes in response to salinity. In this context, compatible solutes such as betaine and trehalose serve as primary osmoprotectants, whereas PHA accumulation is often negatively affected due to the diversion of energy towards compatible solute synthesis. In this study *Thauera*, *Paracoccus*, *Prosthecobacter*, and *SM1A02* increased under P-limiting conditions, potentially limiting PHA accumulation.

Overall, the present findings support the feasibility of using saline-adapted inocula for PHA production, while more detailed mechanistic insights into stress response strategies and functional roles of specific taxa remain to be addressed in future studies.

Conclusion

Using activated sludge from tannery wastewater as inoculum, a PHA-accumulating mixed microbial community was enriched under different selective pressures by varying sequentially the limiting nutrient (N or P). The study investigated PHB accumulation performance and microbial community in a single 1.3 L SBR fed with a synthetic effluent composed of acetic and propionic acids under saline conditions (5 g NaCl L^{-1}) and operated with UF. The results suggest that type of nutrient limitation influences both process performance and microbial community structure. Higher PHB accumulation performance was observed under N compared to P limitation. A hypothesis is that P limitation may have promoted P accumulation phenomena, potentially disrupting the separation between growth and accumulation phases. In alternative, metabolic energy redirection mechanisms may have reduced accumulation.

Changes in microbial community composition were observed under both limiting conditions. Filamentous PHA-associated bacteria, such as *Neomegalonema*, were prevalent under N-limiting conditions and decreased under P-limitation, whereas genera such as *Thauera* and *Paracoccus* increased in relative abundance under P-limitation conditions.

Supplementary Information The online version contains supplementary material available at https://doi.org/10.1007/s13762-026-07412-w.

Acknowledgements This project has received funding from the European Union's Horizon 2020 research and innovation programme under the Marie Skłodowska-Curie grant agreement No 872053, RISE-RECYCLES project.

Funding Open Access funding provided thanks to the CRUE-CSIC agreement with Springer Nature. H2020 Marie Skłodowska-Curie Actions, 872053, David Gabriel

Data availability The sequencing reads used in this study have been deposited in the NCBI GEO (Gene Expression Omnibus) database under the accession GSE263302. Analysis scripts for the bioinformatics processing of reads and for the microbial community analyses are freely available at https://github.com/LeandroD94/Papers/tree/main/2024_PHA_microbiota_N_P_condition

Declarations

Conflict of interest The authors declare that they have no conflict of interest.

Open Access This article is licensed under a Creative Commons Attribution 4.0 International License, which permits use, sharing, adaptation, distribution and reproduction in any medium or format, as long as you give appropriate credit to the original author(s) and the source, provide a link to the Creative Commons licence, and indicate if changes were made. The images or other third party material in this article are included in the article's Creative Commons licence, unless indicated otherwise in a credit line to the material. If material is not included in the article's Creative Commons licence and your intended use is not permitted by statutory regulation or exceeds the permitted use, you will need to obtain permission directly from the copyright holder. To view a copy of this licence, visit http://creativecommons.org/licenses/by/4.0/.

References

Altun M (2019) Polyhydroxyalkanoate production using waste vegetable oil and filtered digestate liquor of chicken manure. Prep Biochem Biotechnol 49:493–500. https://doi.org/10.1080/10826068.2019.1587626

Andreolli M, Scerbacov V, Frison N, Zaccone C, Lampis S (2022) *Thauera* sp. Sel9, a new bacterial strain for polyhydroxyalkanoates production from volatile fatty acids. N Biotechnol 72:71–79. https://doi.org/10.1016/j.nbt.2022.09.004

APHA (1998) Standard methods for the examination of water and wastewater, 20th Edition. American Public Health Association, American Water Works Association and Water Environmental Federation, Washington DC

Argiz L, Fra-Vázquez A, del Río ÁV, Mosquera-Corral A (2020) Optimization of an enriched mixed culture to increase PHA

accumulation using industrial saline complex wastewater as a substrate. Chemosphere. https://doi.org/10.1016/j.chemosphere.2020.125873

Argiz L, Gonzalez-Cabaleiro R, Correa-Galeote D, Val del Rio A, Mosquera-Corral A (2021) Open-culture biotechnological process for triacylglycerides and polyhydroxyalkanoates recovery from industrial waste fish oil under saline conditions. Sep Purif Technol. https://doi.org/10.1016/j.seppur.2021.118805

Bokulich NA, Subramanian S, Faith JJ, Gevers D, Gordon JI, Knight R, Mills DA, Caporaso JG (2013) Quality-filtering vastly improves diversity estimates from Illumina amplicon sequencing. Nat Methods 10:57–59. https://doi.org/10.1038/nmeth.2276

Bolyen E, Rideout JR, Dillon MR et al (2019) Reproducible, interactive, scalable and extensible microbiome data science using QIIME 2. Nat Biotechnol. https://doi.org/10.1038/s41587-019-0209-9

Brison A, Rossi P, Derlon N (2022) Influent carbon to phosphorus ratio drives the selection of PHA-storing organisms in a single CSTR. Water Res X. https://doi.org/10.1016/j.wroa.2022.100150

Cabrera F, Torres-Aravena Á, Pinto-Ibieta F, Campos JL, Jeison D (2021) On-line control of feast/famine cycles to improve PHB accumulation during cultivation of mixed microbial cultures in sequential batch reactors. Int J Environ Res Public Health. https://doi.org/10.3390/ijerph182312611

Callahan BJ, McMurdie PJ, Rosen MJ, Han AW, Johnson AJA, Holmes SP (2016) DADA2: high-resolution sample inference from Illumina amplicon data. Nat Methods 13:581–583. https://doi.org/10.1038/nmeth.3869

Cao Q, Sun X, Rajesh K, Chalasani N, Gelow K, Katz B, Shah VH, Sanyal AJ, Smirnova E (2021) Effects of rare microbiome taxa filtering on statistical analysis. Front Microbiol. https://doi.org/10.3389/fmicb.2020.607325

Carvalho JM, Marreiros BC, Reis MAM (2022) Polyhydroxyalkanoates production by mixed microbial culture under high salinity. Sustainability. https://doi.org/10.3390/su14031346

Cavaillé L, Albuquerque M, Grousseau E, Lepeuple AS, Uribelarrea JL, Hernandez-Raquet G, Paul E (2016) Understanding of polyhydroxybutyrate production under carbon and phosphorus-limited growth conditions in non-axenic continuous culture. Bioresour Technol 201:65–73. https://doi.org/10.1016/j.biortech.2015.11.003

Chen Z, Guo Z, Wen Q, Huang L, Bakke R, Du M (2015) A new method for polyhydroxyalkanoate (PHA) accumulating bacteria selection under physical selective pressure. Int J Biol Macromol 72:1329–1334. https://doi.org/10.1016/j.ijbiomac.2014.10.027

Chen Y, Zhao X, Zhang J, Wang H, Ye Z, Ma W, Mao R, Zhang S, Dahlgren RA, Gao H, Chen Z, Xia S (2025) Combined application of nitrate and schwertmannite promotes As(III) immobilization and greenhouse gas emission reduction in flooded paddy fields. J Environ Chem Eng. https://doi.org/10.1016/j.jece.2025.119845

Clagnan E, Adani F (2023) Influence of feedstock source on the development of polyhydroxyalkanoates-producing mixed microbial cultures in continuously stirred tank reactors. N Biotechnol 76:90–97. https://doi.org/10.1016/j.nbt.2023.05.005

Coats ER, Watson BS, Brinkman CK (2016) Polyhydroxyalkanoate synthesis by mixed microbial consortia cultured on fermented dairy manure: effect of aeration on process rates/yields and the associated microbial ecology. Water Res 106:26–40. https://doi.org/10.1016/j.watres.2016.09.039

Correa-Galeote D, Argiz L, Val Del Rio A, Mosquera-Corral A, Juarez-Jimenez B, Gonzalez-Lopez J, Rodelas B (2022) Dynamics of PHA-accumulating bacterial communities fed with lipid-rich liquid effluents from fish-canning industries. Polymers (Basel). https://doi.org/10.3390/polym14071396

Crognale S, Tonanzi B, Valentino F, Majone M, Rossetti S (2019) Microbiome dynamics and phaC synthase genes selected in a pilot plant producing polyhydroxyalkanoate from the organic fraction of urban waste. Sci Total Environ 689:765–773. https://doi.org/10.1016/j.scitotenv.2019.06.491

Cruz RAP, Oehmen A, Reis MAM (2022) The impact of biomass withdrawal strategy on the biomass selection and polyhydroxyalkanoates accumulation of mixed microbial cultures. N Biotechnol 66:8–15. https://doi.org/10.1016/j.nbt.2021.08.004

Cui YW, Zhang HY, Lu PF, Peng YZ (2016) Effects of carbon sources on the enrichment of halophilic polyhydroxyalkanoate-storing mixed microbial culture in an aerobic dynamic feeding process. Sci Rep. https://doi.org/10.1038/srep30766

Di Caprio F (2022) A fattening factor to quantify the accumulation ability of microorganisms under N-starvation. N Biotechnol 66:70–78. https://doi.org/10.1016/j.nbt.2021.04.001

Di Gloria L, Casbarra L, Bastiani M, Memoli G, Ramazzotti M (2025) Human DNA hijacking microbiota surveys: causes and consequences in colon related 16s rRNA amplicon sequencing. Gut Microbiome. https://doi.org/10.1017/gmb.2025.10012

Dias JML, Oehmen A, Serafim LS, Lemos PC, Reis MAM, Oliveira R (2008) Metabolic modelling of polyhydroxyalkanoate copolymers production by mixed microbial cultures. BMC Syst Biol. https://doi.org/10.1186/1752-0509-2-59

Estévez-Alonso Á, Pei R, van Loosdrecht MCM, Kleerebezem R, Werker A (2021) Scaling-up microbial community-based polyhydroxyalkanoate production: status and challenges. Bioresour Technol. https://doi.org/10.1016/j.biortech.2021.124790

Franklin O, Hall EK, Kaiser C, Battin TJ, Richter A (2011) Optimization of biomass composition explains microbial growth-stoichiometry relationships. Am Nat. https://doi.org/10.1086/657684

Jayalath SU, de Alwis AP (2025) PHA, the greenest plastic so far: advancing microbial synthesis, recovery, and sustainable applications for circularity. ACS Omega. https://doi.org/10.1021/acsomega.5c00684

Khor JW, Yoon LW, Nguyen-Huynh TT, Ng WL, Low JH (2023) Effect of pH control and uncoupled carbon and nitrogen feeding strategy on enrichment of mixed microbial culture for polyhydroxyalkanoates production. In: Journal of physics: conference series. Institute of physics. https://doi.org/10.1088/1742-6596/2523/1/012001

Korkakaki E, van Loosdrecht MCM, Kleerebezem R (2017) Impact of phosphate limitation on PHA production in a feast-famine process. Water Res 126:472–480. https://doi.org/10.1016/j.watres.2017.09.031

Kragelund C, Nielsen JL, Thomsen TR, Nielsen PH (2005) Ecophysiology of the filamentous Alphaproteobacterium *Meganema perideroedes* in activated sludge. FEMS Microbiol Ecol 54:111–112. https://doi.org/10.1016/j.femsec.2005.03.002

Kunacheva C, Stuckey DC (2014) Analytical methods for soluble microbial products (SMP) and extracellular polymers (ECP) in wastewater treatment systems: a review. Water Res. https://doi.org/10.1016/j.watres.2014.04.044

Lahti L, Shetty S (2017) Tools for microbiome analysis in R. R package. Bioconductor https://doi.org/10.18129/B9.bioc.microbiome

Lang S, Liu L, Li Z, Liu S, Liang J, Lu L, Wang L (2025) Untargeted metabolomics reveals phenolic compound dynamics during mung bean fermentation. Food Chem X. https://doi.org/10.1016/j.fochx.2025.103189

Legendre P, Legendre L (2012) Ecological resemblance. In: Numerical ecology. https://doi.org/10.1016/B978-0-444-53868-0.50007-1

Liu J, Wang Y, Li Y, Peñuelas J, Zhao Y, Sardans J, Tetzlaff D, Liu J, Liu X, Yuan H, Li Y, Chen J, Wu J (2023) Soil ecological stoichiometry synchronously regulates stream nitrogen and phosphorus concentrations and ratios. Catena (Amst). https://doi.org/10.1016/j.catena.2023.107357

Lorini L, di Re F, Majone M, Valentino F (2020) High rate selection of PHA accumulating mixed cultures in sequencing batch reactors with uncoupled carbon and nitrogen feeding. N Biotechnol 56:140–148. https://doi.org/10.1016/j.nbt.2020.01.006

Love MI, Huber W, Anders S (2014) Moderated estimation of fold change and dispersion for RNA-seq data with DESeq2. Genome Biol. https://doi.org/10.1186/s13059-014-0550-8

Mai J, Kockler K, Parisi E, Chan CM, Pratt S, Laycock B (2024) Synthesis and physical properties of polyhydroxyalkanoate (PHA)-based block copolymers: a review. Int J Biol Macromol. https://doi.org/10.1016/j.ijbiomac.2024.130204

Mannina G, Presti D, Montiel-Jarillo G, Carrera J, Suárez-Ojeda ME (2020) Recovery of polyhydroxyalkanoates (PHAs) from wastewater: a review. Bioresour Technol. https://doi.org/10.1016/j.biortech.2019.122478

Martin M (2011) CUTADAPT removes adapter sequences from high-throughput sequencing reads. Embnet J. https://doi.org/10.14806/ej.17.1.200

Matos M, Cruz RAP, Cardoso P, Silva F, Freitas EB, Carvalho G, Reis MAM (2021) Sludge retention time impacts on polyhydroxyalkanoate productivity in uncoupled storage/growth processes. Sci Total Environ. https://doi.org/10.1016/j.scitotenv.2021.149363

Mazzoli L, Munz G, Lotti T, Ramazzotti M (2020) A novel universal primer pair for prokaryotes with improved performances for anammox containing communities. Sci Rep. https://doi.org/10.1038/s41598-020-72577-4

McIlroy SJ, Lapidus A, Thomsen TR, Han J, Haynes M, Lobos E, Huntemann M, Pati A, Ivanova NN, Markowitz V, Verbarg S, Woyke T, Klenk HP, Kyrpides N, Nielsen PH (2015) High quality draft genome sequence of *Meganema perideroedes* str. Gr1T and a proposal for its reclassification to the family Meganemaceae fam. nov. Stand Genomic Sci. https://doi.org/10.1186/s40793-015-0013-1

McMurdie PJ, Holmes S (2013) Phyloseq: an R package for reproducible interactive analysis and graphics of microbiome census data. PLoS ONE. https://doi.org/10.1371/journal.pone.0061217

Montiel-Jarillo G, Carrera J, Suárez-Ojeda ME (2017) Enrichment of a mixed microbial culture for polyhydroxyalkanoates production: effect of pH and N and P concentrations. Sci Total Environ 583:300–307. https://doi.org/10.1016/j.scitotenv.2017.01.069

Moretto G, Lorini L, Pavan P, Crognale S, Tonanzi B, Rossetti S, Majone M, Valentino F (2020) Biopolymers from urban organic waste: influence of the solid retention time to cycle length ratio in the enrichment of a mixed microbial culture (MMC). ACS Sustain Chem Eng. https://doi.org/10.1021/acssuschemeng.0c04980

Munz G, Gori R, Cammilli L, Lubello C (2008) Characterization of tannery wastewater and biomass in a membrane bioreactor using respirometric analysis. Bioresour Technol 99:8612–8618. https://doi.org/10.1016/j.biortech.2008.04.004

Oksanen J et al (2024) vegan: community ecology package. R package. https://cran.r-project.org/web/packages/vegan/index.html

Oliveira CSS, Silva CE, Carvalho G, Reis MA (2017) Strategies for efficiently selecting PHA producing mixed microbial cultures using complex feedstocks: feast and famine regime and uncoupled carbon and nitrogen availabilities. N Biotechnol 37:69–79. https://doi.org/10.1016/j.nbt.2016.10.008

Palmeiro-Sánchez T, Fra-Vázquez A, Rey-Martínez N, Campos JL, Mosquera-Corral A (2016a) Transient concentrations of NaCl affect the PHA accumulation in mixed microbial culture. J Hazard Mater 306:332–339. https://doi.org/10.1016/j.jhazmat.2015.12.032

Palmeiro-Sánchez T, Oliveira CSS, Gouveia AR, Noronha JP, Ramos AM, Mosquera-Corral A, Reis MAM (2016b) NaCl presence and purification affect the properties of mixed culture PHAs. Eur Polym J 85:256–265. https://doi.org/10.1016/j.eurpolymj.2016.10.035

Parte AC, Carbasse JS, Meier-Kolthoff JP, Reimer LC, Göker M (2020) List of prokaryotic names with standing in nomenclature (LPSN) moves to the DSMZ. Int J Syst Evol Microbiol 70:5607–5612. https://doi.org/10.1099/ijsem.0.004332

Quast C, Pruesse E, Yilmaz P, Gerken J, Schweer T, Yarza P, Peplies J, Glöckner FO (2013) The SILVA ribosomal RNA gene database project: improved data processing and web-based tools. Nucleic Acids Res. https://doi.org/10.1093/nar/gks1219

Quinn TP, Erb I, Gloor G, Notredame C, Richardson MF, Crowley TM (2019) A field guide for the compositional analysis of any-omics data. Gigascience. https://doi.org/10.1093/gigascience/giz107

Roibás-Rozas A, Val del Rio A, Hospido A, Mosquera-Corral A (2021) Strategies for the valorisation of a protein-rich saline waste stream into polyhydroxyalkanoates (PHA). Bioresour Technol. https://doi.org/10.1016/j.biortech.2021.124964

Rosenboom JG, Langer R, Traverso G (2022) Bioplastics for a circular economy. Nat Rev Mater. https://doi.org/10.1038/s41578-021-00407-8

Silva F, Campanari S, Matteo S, Valentino F, Majone M, Villano M (2017) Impact of nitrogen feeding regulation on polyhydroxyalkanoates production by mixed microbial cultures. N Biotechnol 37:90–98. https://doi.org/10.1016/j.nbt.2016.07.013

Stouten GR (2021) Exploring microbial diversity extending the boundaries of biopolymer production using parallel cultivation. PhD thesis. https://doi.org/10.4233/uuid:1e63fd37-62af-4dcd-9650-6db0ebfa9ff5

Teoh JH, Soh E, Le Ferrand H (2024) Manipulating fungal growth in engineered living materials through precise deposition of nutrients. Int J Bioprint 10: 168–182. https://doi.org/10.36922/ijb.3939

Thomsen TR, Blackall LL, Aquino de Muro M, Nielsen JL, Nielsen PH (2006) *Meganema perideroedes* gen. nov., sp. nov., a filamentous alphaproteobacterium from activated sludge. Int J Syst Evol Microbiol 56:1865–1868. https://doi.org/10.1099/ijs.0.02916-0

Tian S, Tian Z, Yang H, Yang M, Zhang Y (2017) Detection of viable bacteria during sludge ozonation by the combination of ATP assay with PMA-miseq sequencing. Water. https://doi.org/10.3390/w9030166

Wang X, Oehmen A, Freitas EB, Carvalho G, Reis MAM (2017) The link of feast-phase dissolved oxygen (DO) with substrate competition and microbial selection in PHA production. Water Res 112:269–278. https://doi.org/10.1016/j.watres.2017.01.064

Wang X, Oehmen A, Carvalho G, Reis MAM (2020) Community profile governs substrate competition in polyhydroxyalkanoate (PHA)-producing mixed cultures. N Biotechnol 58:32–37. https://doi.org/10.1016/j.nbt.2020.03.003

Wen Q, Chen Z, Tian T, Chen W (2010) Effects of phosphorus and nitrogen limitation on PHA production in activated sludge. J Environ Sci 22:1602–1607. https://doi.org/10.1016/S1001-0742(09)60295-3

Wen Q, Wang Z, Liu B, Liu S, Huang H, Chen Z (2024) Enrichment performance and salt tolerance of polyhydroxyalkanoates (PHAs) producing mixed cultures under different saline environments. Environ Res 251:118722. https://doi.org/10.1016/j.envres.2024.118722

Zhang Z, Wang Y, Wang X, Zhang Y, Zhu T, Peng L, Xu Y, Chen X, Wang D, Ni BJ, Liu Y (2024) Towards scaling-up implementation of polyhydroxyalkanoate (PHA) production from activated sludge: progress and challenges. J Clean Prod. https://doi.org/10.1016/j.jclepro.2024.141542

Zhou W, Bergsma S, Colpa DI, Euverink GJW, Krooneman J (2023) Polyhydroxyalkanoates (PHAs) synthesis and degradation by microbes and applications towards a circular economy. J Environ Manage. https://doi.org/10.1016/j.jenvman.2023.118033

Zhou J, Lv P, He B, Wu J, Wang G, Ma H, Wang Y, Chen G (2024) Optimisation of the Ethanol Fermentation Process Using Hydrothermal Pretreatment of Cellulose Waste—Effect of Fermentation Pattern and Strain. Molecules. https://doi.org/10.3390/molecules29225266

Publisher's Note Springer Nature remains neutral with regard to jurisdictional claims in published maps and institutional affiliations.